MISS JIN-JU NAM (Orcid ID : 0000-0003-2159-1383)

Article type : Original Article

Ultraviolet- and infrared-induced 11 beta hydroxysteroid dehydrogenase type 1 activating skin photoaging is inhibited by red ginseng extract containing high concentrations of ginsenoside Rg3(S)

Jin-Ju NAM,[1] Ji-Eun MIN, [2] Min-Ho SON, [2] Jin-Hwan OH,[3] and Seunghyun KANG[2*]

[1] R&I Center, COSMAX BTI, Seongnam, Republic of Korea

[2] R&I Center, COSMAX, Seongnam, Republic of Korea

[3] BTGin, Daejeon, Republic of Korea

* Corresponding author: Seunghyun Kang at COSMAX R&I Center, 622, Sampyeong-dong, Bundang-gu, Seongnam-si, Gyeonggi-do, Republic of Korea (13486)

Tel.: 82-31-789-3260

Fax: 82-31-789-3402

E-mail: shyunk@cosmax.com

Running Title: **Red ginseng extract alleviates skin photoaging**

Abstract

Background: Sun irradiation is one of major extrinsic stressors responsible for premature skin aging through activation and expression of 11 beta hydroxysteroid dehydrogenase type 1 (11β-HSD1), which converts inactive cortisone to active cortisol. The aim of this study was to evaluate the inhibitory effects of red ginseng extract containing high concentrations of ginsenoside Rg3(S) (GERg3) on 11β-HSD1-induced skin photoaging.

This article has been accepted for publication and undergone full peer review but has not been through the copyediting, typesetting, pagination and proofreading process, which may lead to differences between this version and the Version of Record. Please cite this article as doi: 10.1111/phpp.12337

Methods: To evaluate the inhibitory effects of GERg3 on ultraviolet (UV) or infrared (IR)-induced skin photoaging, human dermal fibroblasts or a normal human 3D skin model were exposed to UV or an IR. RT-PCR, ELISA, western blot, and H&E staining were used for evaluations. GERg3 was isolated from crude red ginseng.

Results: GERg3 inhibited the increased expressions of 11β-HSD1, interleukin (IL)-6, and matrix metalloproteinase-1 (MMP-1) in UVB- or IR-exposed Hs68 cells. Additionally, the increased cortisol, IL-6, and MMP-1 expressions were effectively reduced by GERg3 in UVA-exposed 3D skin models. The photo-induced decrease of type 1 procollagen also recovered as a result of GERg3 treatment in Hs68 cells and the 3D skin model. In addition, the UVA-exposed dermal thickness was decreased in comparison with the UVA-protected 3D skin model, recovered with GERg3 treatment.

Conclusion: GERg3 had anti-photoaging effects in UV- or IR-exposed human dermal fibroblasts and normal human 3D skin model.

Keywords: Collagen, Ginsenoside Rg3, Hydrocortisone, Skin aging, Sun light

Introduction

Changes of human skin occur with increasing chronological age and even more drastically with repetitive exposure to external stimulations such as sun exposure [1]. Photoaging skin shows phenotypic changes in cutaneous cells and dermal extracellular matrix (ECM) characterized with development of both deep wrinkles and a marked loss of elasticity [1,2]. The 3 major groups of dermal extracellular matrix (ECM) are collagen, elastic fibres, and proteoglycans with oligosaccharides, required for tensile strength, resilience, and hydration, respectively. Collagen is the largest proportion of dermal ECM, which comprises approximately 70%–80% of the dry weight of dermis and has major role in support of skin [3]. In photoaged skin, collagen has degraded, which induces development of dermal atrophy and poor wound healing [3,4]. Actually ultraviolet A (UVA) and ultraviolet B (UVB) radiation stimulate synthesis and activation of matrix metalloproteinases (MMPs), which play an important role in the intense alterations underlying photodamage of the dermal ECM in photoaging and photocarcinogenesis. Specifically, UV-induced MMP-1 and MMP-3 are responsible for the breakdown of interstitial collagen and proteoglycans. Furthermore, UVA- and UVB-mediated induction of cytokine interleukin (IL)-6 increases MMP-1 and MMP-3

protein levels via inter-related autocrine loops [5]. Moreover, infrared (IR) irradiation generates heat, which increases human skin temperature significantly, and heat exposure is widely considered a major extracellular stimuli [6,7]. In fact, heat is involved in premature skin aging processes, which induce an increase in MMP-1 and MMP-3 expression. In addition, the effect of heat exposure on the expression of IL-6 has been investigated, which regulate MMP-1 and MMP-3 expression in an autocrine way as well [7]. Therefore, it is believed that UVA and UVB irradiation, and IR-generated heat, stimulate MMP-1 and MMP-3 expression indirectly through inducing the expression of IL-6 [5,7].

Cortisol is a kind of glucocorticoid (GC), a mammal stress hormone that regulates a wide range of stress responses in humans via the hypothalamo-pituitary-adrenal (HPA) axis [8,9]. Human skin is the organ contributing to the maintenance and regulation of body homeostasis through communication with central nervous and endocrine systems [10-13]. In fact the cells from human skin produce neurohormones, neurotransmitters and neuropeptide [11]. Stressed skin serves elements of the HPA axis such as corticotropin releasing hormone (CRH), proopiomelanocortin (POMC)-derived adrenocorticotropic hormone (ACTH), and finally glucocorticoids as well as their receptors [11,14]. Thus the skin cells, human dermal fibroblasts, melanocytes, and hair follicles are capable of producing cortisol [15,16]. On the other hand in human tissues, cortisol concentration is regulated by an enzyme, 11 beta hydroxysteroid dehydrogenase type 1 (11β-HSD1), which activates cortisol from inactive cortisone [17,18]. Interestingly, cortisol leads to skin aging, including dermal-epidermal junction (DEJ) flattening and reduced number of cells, dermal fibroblast proliferation and collagen production and secretion in human skin [19]. Since 11β-HSD1 is reported to regulate the cortisol secretion, the relation of phenotype between excessive cortisol production and photoaging can be explained by the role of 11β-HSD1 [19]. The expression of 11β-HSD1 has been analyzed in different patterns between photo-exposed and photo-protected human dermal fibroblasts; it has been reported that 11β-HSD1 messenger ribonucleic acid (mRNA) levels were increased in photo-exposed skin as compared with photo-protected skin [20]. In addition, 11β-HSD1-specific inhibitors have effects on increasing dermal collagen content and stimulating fibroblast proliferation [21].

Various kinds of Panax plants have been used in traditional oriental medicine, and among those Panax species, *Panax ginseng* Meyer is one of the most generally used medicinal plants in Asian countries including Korea, China, and Japan [22]. Especially heat-

processed (steamed) *Panax ginseng* (red ginseng) contains ginsenoside Rg3, one of the major ginsenosides, which has antioxidant, anti-tumor, anti-melanogenesis, hair growth, and anti-aging effects in human skin [22–26]. In addition, ginsenoside Rg3 alleviates deleterious GC action in brain and may be beneficial for stress-related brain disorders [27].

In this study, we aim to demonstrate that GERg3 alleviated skin photoaging induced by skin stress. Thus, we investigated whether GERg3 reduced dermal alterations induced by increased 11β-HSD1 expression in UV- or IR-exposed dermal fibroblasts and normal human 3D skin model in vitro.

Materials and Methods

GERg3 production and sample preparation. Dried red ginseng was extracted with 50% (v/v) ethanol in distilled water at 50 °C. The extract was concentrated at 4 °C using rotary evaporators under reduced pressure. The initial extract then underwent a second extraction process with 80–85% ethanol in distilled water at 50 °C and was concentrated at 4 °C using rotary evaporators. The second extract was combined with citric acid, to increase ginsenoside Rg3(S), and purified by column chromatography. Red ginseng extract containing high concentrations of ginsenoside Rg3(S) (GERg3) was finally dried using a spray drier. Total ginsenoside Rg3(S) in the extracted power was composed of up to 14%. The resulting GERg3 was suspended in dimethyl sulfoxide and diluted to 0.1 and 1 ppm concentrations in dimethyl sulfoxide (DMSO) for experimental procedures.

Chemicals and reagents for HPLC analysis. Methanol (HPLC grade, Sigma-Aldrich Corp., St. Louis, MO, USA) was purchased. Ultrapure water for HPLC analysis obtained from Milli-Q direct (16Milli-Q system, MerckMillipore Corp., Darmstadt, Germany). The standard reagent was Ginsenoside Rg3(S) (ChromaDex, Irvine, CA, USA).

Apparatus. HPLC analysis of Ginsenoside Rg3(S) was processed in Agilent HPLC-DAD system (Agilent 1260 series, Agilent Technologies, Santa Clara, CA, USA). The HPLC-DAD system consisted of a 1260 quaternary pump, 1260 autosampler and 1260 diode array detector and these were controlled by OpenLAB CDS Chemstation edition (Agilent Technologies, Santa Clara, CA, USA). Phenomenex Gemini-C18 column (4.6 × 250 mm, 5 μm, Phenomenex Inc., Torrance, CA, USA) was used for analysis.

HPLC analysis. With the apparatus explained above, HPLC analysis data was acquired at 203 nm for UV/Vis detection wavelength. The injection volume was 10 μL. A binary water (solvent A) and acetonitrile (solvent B) gradient was used for elution and the flow rate was 1.0 mL per min. The gradient conditions are 80 % solvent A and 20 % solvent B for 5 min, followed by a gradient to 77% A and 23 % B for 15 min, followed by a gradient to 70 % A and 30 % B for 5 min, followed by a gradient to 60 % A and 40 % B for 5 min, followed by a gradient to 50 % A and 50 % B for 5 min, followed by a gradient to 15 % A and 85 % B for 25 min and keep for 2 min, followed by a gradient to 80 % A and 20 % B for 3 min and keep for 5 min.

Cell culture. Human dermal fibroblasts (Hs68) were purchased from the American Type Culture Collection (ATCC; Manassas, VA, USA). The Hs68 cells were cultured in Dulbecco's modified Eagle's medium (DMEM; HyClone Laboratories, Inc., Logan, UT, USA), supplemented with 1% antibiotic-antimycotic (HyClone Laboratories, Logan, UT, USA) and 10% fetal bovine serum (HyClone Laboratories, Logan, UT, USA) in an atmosphere of 5% carbon dioxide (CO_2) at 37 °C. The cells were transferred to 150 mm plates at 80% confluence as required.

Normal human 3D skin model culture. A normal human 3D skin model at full thickness (Epiderm-FT; MatTek Co., Ashland, MA, USA), comprising normal human keratinocytes and normal human fibroblasts, was cultured. The tissue was transferred to 6-well plates and cultured in DMEM (MatTek Co., Ashland, MA, USA) containing 5 μg/mL gentamicin B (MatTek Co., Ashland, MA, USA), 0.25 μg/mL amphotericin B (MatTek Co., Ashland, MA, USA), and other growth factors, in an atmosphere of 5% CO_2 at 37 °C overnight.

Ultraviolet exposure and sample treatment. For UV irradiation, the Hs68 cells were seeded (4×10^5 cells/well) at 80% confluence, and the normal human 3D skin model was stabilized into 6-well plates and incubated in an atmosphere of 5% CO_2 at 37 °C overnight. To evaluate the detrimental effects of UVA and UVB radiation on skin, the cells and the normal human 3D skin model were exposed to UVA (365 nm) or UVB (302 nm) crosslinker (UVP, Upland, CA, USA). The cells were irradiated with UVB light (15 mJ/cm^2) and then GERg3 and PF915275 (PF; SANTA CRUZ Biotechnology, Dallas, TX, USA) were treated to the cells in serum-free medium. The stabilized normal human 3D skin tissue model was irradiated with UVA light (40 J/cm^2). After UVA irradiation, the tissues were treated with samples.

IR exposure and sample treatment. For IR irradiation, the Hs68 cells were seeded (4×10^5 cells/well), and the normal human 3D skin model was stabilized in 6-well plates at 80% confluence and incubated in 5% CO_2 at 37 °C overnight. Also, to evaluate the detrimental effects of IR and IR-generated heat on skin alterations, the cells and the normal human 3D skin model were exposed to an IR lamp (Daekyung Co. Ltd., Pocheon, South Korea) emitting light at 600–1200 nm. Six-well plates with lids were placed 20 cm under an IR lamp for 15 min. (The distance from the lids of the plates to the surface of the media, 2 mL per well, was 1.5 cm.) The cells and the 3D skin were exposed to the radiation with a final media temperature of 41 °C. An IR thermometer, GM550 (Benetech Co. Ltd., China), was used to measure the surface temperature of the tissue. After IR irradiation, the cells and the tissues were treated with samples.

Real-time reverse transcriptase-polymerase chain reaction (real-time RT-PCR). Hs68 cells were harvested after 24 h UVB or IR exposure and sample treatment. The total RNA was extracted from the cultured cell pellet using a TRIzol reagent (RNAiso; Takara, Shiga, Japan) and quantified using spectrophotometry at 260 nm. Equal amounts of RNA (2 μg) were reverse transcribed using Reverse Transcription Premix (ELPIS-Biotech, Inc., Daejeon, South Korea). The complementary deoxyribonucleic acid (cDNA) products were amplified using polymerase chain reaction (PCR) with a SYBR green master mix (Applied Biosystems, Waltham, MA, USA). They were then analyzed using specific primers (Bioneer Corp., Daejeon, South Korea): β-actin forward 5′-GGCCATCTCTTGCTCGAAGT-3′, β-actin reverse 5′-GAGACCTTCAACACCCCAGC-3′; 11β-HSD1 forward 5′-AAGCAGAGCAATGGAAGCAT-3′, 11β-HSD1 reverse 5′-GAAGAACCCATCCAAAGCAA-3′; IL-6 forward 5′- TACCCCCAGGAGAAGATTCC-3′, IL-6 reverse 5′- TTTTCTGCCAGTGCCTCTTT-3′; MMP-1 forward 5′-AAGCGTGTGACAGTAAGCTA-3′, MMP-1 reverse 5′- AACCGGACTTCATCTCTG-3′; col1α1 forward 5′- CTCGAGGTGGACACCACCCT -3′, and col1α1 reverse 5′-CAGCTGGATGGCCACATCGG -3′. Before PCR was performed, the primers were denatured at 94 °C for 5 min. The amplification process consisted of over 40 cycles: denaturation at 95 °C for 30 s, annealing at 50 °C for 1 min, and extension at 72 °C for 1 min. The StepOnePlus (Applied Biosystems, Waltham, MA, USA) was used for RT-PCR, and β-actin was used as a reference gene.

Enzyme-linked immunosorbent assay (ELISA). The Hs68 cells were harvested after 24 h

UVB or IR exposure and sample treatment. Normal human 3D skin model was harvested after 48-h UVA exposure and sample treatment. Culture media from the cultured Hs68 cells was used to measure the secreted cortisol, IL-6, and type 1 procollagen. Culture media from the cultured normal human 3D skin model was used to measure the secreted cortisol, IL-6, MMP-1, and type 1 procollagen. The collected media was separated from impurities by centrifugation at 13,500 × *g* for 10 min. Cortisol, IL-6, MMP-1, and type 1 procollagen secretion were measured using the cortisol enzyme-linked immunosorbent assay kit (R&D systems, Minneapolis, MN, USA), IL-6 ELISA kit (Life Technologies, Grand Island, NY, USA), MMP-1 ELISA kit (Abcam, Cambridge, UK), and Type 1 procollagen EIA kit (Takara Bio Inc., Otsu, Japan), respectively. The assays were performed following the manufacturers' instructions.

Western blot analysis. The Hs68 cells were harvested after 48 h of UVB or IR exposure and sample treatment. Cells were lysed in a radioimmunoprecipitation assay lysis buffer (Sigma-Aldrich Corp., St. Louis, MO, USA). For western blotting analysis, protein-matched samples (using the Bradford assay) were electrophoresed using sodium dodecyl sulfate polyacrylamide gel electrophoresis and then transferred to polyvinylidene fluoride membranes. The polyvinylidene fluoride membranes were blocked with 5% skim milk at room temperature for 1 h and then incubated with primary antibodies of β-actin and MMP-1 (1:1000 dilution; Abcam, Cambridge, UK). Bound antibodies were detected with a horseradish peroxidase–conjugated secondary antibody (1:5000 dilution; Bethyl Laboratories, Inc., Montgomery, TX, USA). Signals were detected with the enhanced chemiluminescence detection system (Thermo Fisher Scientific, Rockford, IL, USA) and visualized using the G:Box Chemi system (Syngene, Cambridge, UK).

Hematoxylin and eosin (H&E) staining. Forty-eight hours after UVA exposure and sample treatment, hematoxylin & eosin (H&E) staining and dermal thickness measurement were performed. Then, 5 μm paraffin-embedded normal human 3D skin model (Epiderm-FT, MatTek Corporation, Ashland, MA, USA) sections were deparaffinised and rehydrated with xylene and ethanol. The sections were stained with hematoxylin to visualize the nuclei in purple. Eosin staining was then performed to classify the cytosolic area in red. The stained sections were observed under a light microscope. The dermal thickness of the skin tissue was measured on the photographs using iSolution Lite software (Advanced Imaging Concepts, Princeton, NJ, USA).

Statistics. The in vitro data are expressed as the mean ± standard deviation (SD) of at least three independent experiments. All data were compared with a T-test. The analysis was performed using SPSS version 19.0 (SPSS Inc., Chicago, IL, USA). P-values less than 0.05 were considered to be statistically significant and were marked as follows: #p<0.05, and ##p>0.01 (normal vs. UV or IR control), *p<0.05, and **p<0.01 (UV or IR control vs. sample-treated group).

Results

Identification of Rg3(S) of GERg3. Chromatograms of ginsenoside Rg3(S) of the standard reagent and extracted powder are shown in Supp. Fig. 1A and Supp. Fig. 1B. By comparing both the retention time on chromatogram and UV spectra of these HPLC data, it was identified that the extracted powder contain the high concentration of ginsenoside Rg3(S) and the concentration is about 14 %. The UV spectra of Rg3(S) is shown in Supp. Fig. 1C. Because the range of detection wavelength was from 190 nm to 400 nm and the maximum absorption was shown near 190 nm, the wavelength that Rg3(S) was detected was selected for 203 nm considering the capacity of the diode array detector.

Inhibitory effect of GERg3 on UVB-induced stress reaction. To investigate whether GERg3 inhibits the UVB-induced stress reaction, human dermal fibroblasts (Hs68) were exposed to 15 mJ/cm^2 UVB. As a result, 11β-HSD1 expression was inhibited by GERg3 in UVB-irradiated Hs68 cells in a dose dependent manner (Fig. 1A). Moreover, though cortisol secretion increased in UVB-irradiated Hs68 cells, GERg3 inhibited the cortisol secretion (Fig. 1B). These results suggest that GERg3 inhibits the stress reaction that is caused by UVB-induced increase of 11β-HSD1 expression and cortisol concentration in human dermal fibroblasts.

Inhibitory effect of GERg3 on UVB-induced dermal ECM alteration. To investigate whether GERg3 inhibits UVB-induced dermal ECM alteration, Hs68 cells were exposed to 15 mJ/cm^2 of UVB. We found that IL-6 mRNA expression and protein secretion were inhibited by GERg3 in UVB-irradiated Hs68 cells in a dose dependent manner (Fig. 2A, B). We also found that MMP-1 mRNA and protein expression were inhibited by GERg3 in a dose dependent manner (Fig. 2C, D). We also found dose-dependent recovery of type 1 procollagen mRNA and protein expression in UVB-irradiated Hs68 cells treated with GERg3

(Fig. 2E, F). Procollagen mRNA and protein expression combine to represent dermal ECM, and are regulated by IL-6 and MMP-1.

Inhibitory effect of GERg3 on IR-induced stress reaction. To investigate whether GERg3 inhibits IR-induced stress reaction, Hs68 cells were exposed to a final temperature of 41 ℃. As a result, 11β-HSD1 expression was inhibited by GERg3 in IR-irradiated Hs68 cells in a dose dependent manner (Fig. 3A). Moreover, cortisol secretion increased in IR-irradiated Hs68 cells, but GERg3 inhibited the cortisol secretion (Fig. 3B). These results suggest that GERg3 inhibits the stress reaction that was increased by the IR-induced increase of 11β-HSD1 expression and cortisol concentration in human dermal fibroblasts.

Inhibitory effect of GERg3 on IR-induced dermal ECM alteration. To investigate whether GERg3 inhibits IR-induced dermal ECM alteration, Hs68 cells were exposed to a final temperature of 41 ℃. As a result, IL-6 mRNA expression and protein secretion were inhibited by GERg3 in IR-irradiated Hs68 cells in a dose dependent manner (Fig. 4A, B). In addition, MMP-1 mRNA and protein expression were inhibited by GERg3 in IR-irradiated Hs68 cells in a dose dependent manner (Fig. 4C, D). Finally, type 1 procollagen mRNA and protein expression, which represent dermal ECM, and are altered by IL-6 and MMP-1, recovered as a result of GERg3 treatment in IR-irradiated Hs68 cells in a dose dependent manner (Fig. 4E, F).

Inhibitory effect of GERg3 on UVA-induced 3D skin alteration. 11β-HSD1 expression in the UVB- or IR-exposed human dermal fibroblasts led to an increase in cortisol concentration, resulting in decreased dermal ECM. We next investigated the effect of GERg3 on cortisol concentration, IL-6 secretion, and MMP-1 expression in the normal human 3D skin model exposed to 40 J/cm^2 of UVA radiation (Fig. 5A, B, C). We also found that alteration of dermal thickness is assisted by a decrease in dermal ECM. UVA was associated with a decrease in the recovery of type 1 procollagen with GERg3 treatment (Fig. 5D). Finally, UVA-exposed skin tissue displayed decreased dermal thickness with noticeable atrophy compared to the UVA-protected tissue. We observed a recovery of dermal thickness in the UVA-exposed 3D skin model with GERg3 treatment (Fig. 5E).

Discussion

Excessive sun exposure to human skin induces wrinkles, cancer, erythema, and pigmentation, through alterations in numerous pathways [28–31]. Also it is known that skin stress resulting from excessive sun exposure has harmful effects on human skin [29]. Our study demonstrated that GERg3 significantly protected dermal matrix in UVB- or IR-irradiated human dermal fibroblasts and a UVA-irradiated normal human 3D skin model. Based on the results of this study, we conclude that GERg3 is effective in alleviating skin stress induced by UV and IR irradiation.

GCs are produced and secreted by adrenal cortex. Cytochrome P450 (CYP11A1) is the enzyme for catalysis of the cleavage of the side chain of cholesterol to produce pregnenolone, finally the precursor of GCs [32]. Stressful environmental changes activate and elevate the GCs concentration [8,9]. Human skin is an independent steroidogenic organ to maintain local homeostasis against harmful attack of external environment and biological factors [33,34]. Thus human skin and hair are affected sensitively by stress reaction, and they produce GCs through their own peripheral neuroendocrine systems [35]. Topical application of cortisol has been used for dermatologic therapy because of its potent anti-inflammatory and anti-proliferative effects [36]. However, application of topical cortisol been shown to reduce collagen synthesis in human skin, contributing to skin atrophy [37]. 11β-HSD1 was identified for the enzyme interconverting cortisol and cortisone. Thus, 11β-HSD1 has been attentioned as a therapeutic target because of its association with elevated cortisol activation [38]. UV radiation, as an environmental stress inducer stimulates expression of 11β-HSD1, 11β-HSD2, and glucocorticoid receptor (GR) genes and protein, and cortisol secretion as well [29]. In addition, 11β-HSD1 activity and expression are elevated in photo-exposed skin tissues. It has been demonstrated that 11β-HSD1 is a potent indicator of photoaging [19]. Our findings showed that 11β-HSD1 expression was increased in UVB- or IR-irradiated Hs68 cells and GERg3 decreased 11β-HSD1 expression in UVB- or IR-irradiated Hs68 cells. In addition, cortisol level was reduced by GERg3 in both UVB- and IR-irradiated Hs68 cells. It is suggested that GERg3 can reduce stress reaction in human dermal fibroblasts.

Photo-damaged skin presents a reduction of type 1 procollagen synthesis. MMP-1 has a primary role in most of the collagen damage in photoaged skin, and increased MMP-1 expression is closely related with collagen degradation [4]. UVA and UVB induce MMP-1 activity and thus contribute to damage of dermis through enhancing IL-6 synthesis and secretion [5,39,40]. In addition, recent studies indicate that IR and IR-induced heat stimulate skin aging similarly to UV radiation [41]. In fact, heat also induces both mRNA and protein

levels of MMP-1 and MMP-3 expression by an IL-6 dependent manner [7]. In the current study, we investigated whether GERg3 could inhibit skin photoaging induced by the increase of 11β-HSD1 expression. Applying PF915275 (PF) as a specific inhibitor of 11β-HSD1, to the human dermal fibroblasts and normal human 3D skin model decreased photo-induced cortisol, IL-6, and MMP-1, and resulted recovery of collagen production and dermal thickness. In addition, GERg3 treated photo-exposed human dermal fibroblasts and normal human 3D skin model decreased photo-induced cortisol, IL-6, and MMP-1, and resulted recovery of collagen production and dermal thickness the same as PF. In fact, inhibition of 11β-HSD1 positively regulates collagen metabolism by increasing the number of dermal fibroblasts [21]. Moreover, 11β-HSD1 mediated pro-inflammatory responses in macrophages, and inhibition of 11β-HSD1 decreased TNF-α-induced IL-6 expression in human epidermal keratinocytes [42].

In general, red ginseng and ginsenosides derived from red ginseng are well known for their beneficial effects on human body [43]. Among the ginsenosides, Rg3 presents an anti-photoaging effect in human skin by decreasing UVB-induced MMP-2 activity. Moreover 20(S)-Rg3, which is an isoform of Rg3, has an inhibitory effect on UVB-induced MMP-2 activity, implying a skin anti-photoaging activity more than 20(R)-Rg3 do [23]. Thus we developed GERg3 to use an anti-aging ingredient. We found that GERg3 had inhibitory effects on skin photoaging through the down-regulation of photo-induced 11β-HSD1 expression.

In conclusion, GERg3 inhibited skin photoaging and aided in recovery of photo-induced dermal damage, in addition to suppressing photo-induced increase of IL-6 and MMP-1 levels in UV- and IR-exposed human dermal fibroblasts and normal human 3D skin model. In addition, our results suggested that GERg3 could alleviate the photo-induced increase of cortisol secretion through the increase of 11β-HSD1 expression, which could be a cause of the skin photoaging response.

Acknowledgement

This study was supported by a Grant of the Korea Healthcare Technology R & D Project, Ministry of Health & Welfare, Republic of Korea (Grant No. HN12C0061(A103017)).

References

[1] Naylor E C, Watson R E B, Sherratt M J. Molecular aspects of skin ageing. Maturitas 2011: 69: 249–256.

[2] Theocharis A D, Skandalis S S, Gialeli C, Karamanos N K. Extracellular matrix structure. Adv Drug Deliv Rev 2016: 97: 4–27.

[3] Waller J M, Maibach H I. Age and skin structure and function, a quantitative approach (II): protein, glycosaminoglycan, water, and lipid content and structure. Skin Res Technol 2006: 12: 145–154.

[4] Varani J, Perone P, Fligiel S E G, Fisher G J, Voorhees JJ. Inhibition of type I procollagen production in photodamage: correlation between presence of high molecular weight collagen fragments and reduced procollagen synthesis. J Invest Dermatol 2002: 199: 12–19.

[5] Brenneison P, Wlaschek M, Wenk J et al. Ultraviolet-B induction of interstitial collagenase and stromelyn-1 occurs in human dermal fibroblasts via an autocrine interleukin-6-dependent loop. FEBS Lett 1999: 449: 36–40.

[6] Schieke S M, Schroeder P, Krutmann J. Cutaneous effects of infrared radiation: From clinical observations to molecular response mechanisms. Photodermatol Photoimmunol Photomed 2003: 19: 228–234.

[7] Park C H, Lee M J, Ahn J et al. Heat shock-induced matrix metalloproteinase (MMP)-1 and MMP-3 are mediated through ERK and JNK activation and via an autocrine interleukin-6 loop. J Invest Dermatol 2004: 123: 1012–1019.

[8] Zoumakis E, Kalantaridou S N, Chrousos G P. The “brain-skin connection”: nerve growth factor-dependent pathways for stress-induced skin disorders. J Mol Med 2007: 85: 1347–1349.

[9] Chen Y, Lyga J. Brain-skin connection: stress, inflammation and skin aging. Inflamm Allergy Drug Targets 2014: 13: 177–190.

[10] Slominski A, Ermak G, MIHM M. ACTH receptor, CYP11A1, CYP17 and CYP21A2 genes are expressed in skin. J Clin Endocrinol Met 1996: 81: 2746-2749.

[11] Slominski A T, Manna P R, Tuckey R C. On the role of skin in the regulation of local and systemic stroidogenic activities. Steroids 2015: 103: 72-88.

[12] Slominski A T, Zmijewski M A, Zbytek B, Tobin D J, Theoharides T C, Rivier J. Key role of CRF in the skin stress response system. Endocr Rev 2013: 34: 827-884.

[13] Slominski A, Wortsman J, Luger T, Paus R, Solomon S. Corticotropin releasing hormone and proopiomelanocortin involvement in the cutaneous response to stress. Physiol

Rev 2000: 80: 979-1020.

[14] Skobowiat C, Dowdy J C, Sayre R M, Tuckey R C, Slominski A. Cutaneous hypothalamic-pituitary-adrenal axis homolog: regulation by ultraviolet radiation. Am J Physiol Endocrinol Metab 2011: 301: E484-E493.

[15] Slominski A, Zbytek B, Szczesniewski A, Semak I, Kaminski J, Sweatman T, Wortsman J. CRH stimulation of corticosteroids production in melanocytes is mediated by ACTH. Am J Physiol Endocrinol Metab 2005: 288: E701-E706.

[16] Slominski A, Zbytek B, Szczesniewski A, Wortsman J. Cultured human dermal fibroblasts do produce cortisol. J Invest Dermatol 2006: 126: 1177-1178.[17] Odermatt A, Klusonova P. 11β-hydroxysteroid dehydrogenase 1: regeneration of active glucocorticoids is only part of the story. J Steroid Biochem Mol Biol 2015: 151: 85–92.

[18] Odermatt A, Atanasov A G, Balazs Z et al. Why is 11β-hydroxysteroid dehydrogenase type 1 facing the endoplasmic reticulum lumen?: Physiological relevance of the membrane topology of 11β-HSD1. Mol Cell Endocrinol 2006: 248: 15–23.

[19] Tiganescu A, Tahrani A A, Morgan S A et al. 11β-hydroxysteroid dehydrogenase blockade prevents age-induced skin structure and function defects. J Clin Invest 2013: 123: 3051–3060.

[20] Tiganescu A, Walker E A, Hardy R S, Mayes A E, Stewart P M. Localization, age- and site-dependent expression, and regulation of 11β-hydroxysteroid dehydrogenase type 1 in Skin. J Invest Dermatol 2011: 131: 30–36.

[21] Terao M, Tani M, Itoi S et al. 11β-hydroxysteroid dehydrogenase 1 specific inhibitor increased dermal collagen content and promotes fibroblast proliferation. PloS one 2014: 9: e93051.

[22] Surh Y J, Na H K, Lee J Y, Keum Y S. Molecular mechanisms underlying anti-tumor promoting activities of heat-processed Panax ginseng C.A. Meyer. J Korean Med Sci 2001: Suppl: S38-41.

[23] Lim C J, Choi W Y, Jung H J. Stereoselective skin anti-photoaging properties of ginsenoside Rg3 in UV-B-irradiated keratinocytes. Biol Pharm Bull 2014: 37: 1583–1590.

[24] Shin D H, Cha Y J, Yang K E et al. Ginsenoside Rg3 up-regulates the expression of vascular endothelial growth factor in human dermal papilla cells and mouse hair follicles. Phytother Res 2014: 28: 1088–1095.

[25] Keum Y S, Han S S, Chun K S et al. Inhibitory effects of the ginsenoside Rg3 on phorbol ester-induced cyclooxygenase-2 expression, NF-κB activation and tumor promotion. Mutat Res 2003: 523-524: 75-85.

[26] Lee S J, Lee W J, Chang S E, Lee G Y. Antimelanogenic effect of ginsenoside Rg3 through extracellular signal-regulated kinase-mediated inhibition of microphthalmia-associated transcription factor. J Ginseng Res 2015: 39: 238–242.

[27] Kim S O, You J M, Yun S J et al. Ginsenoside Rb1 and Rg3 attenuate glucocorticoid-induced neurotoxicity. Cell Mol Neurobiol 2010: 30: 857–862.

[28] Clydesdale G J, Dandie G W, Muller H K. Ultraviolet light induced injury: immunological and inflammatory effects. Immunol Cell Biol 2001: 79: 547–568.

[29] Skobowiat C, Sayre R M, Dowdy J C, Slominski A T. Ultraviolet radiation regulates cortisol activity in a waveband-dependent manner in human skin ex vivo. Br J Dermatol 2013: 168: 595–601.

[30] Chung I, Lee J, Park Y S et al. Inhibitory mechanism of Korean Red Ginseng on GM-CSF expression in UVB-irradiated keratinocytes. J Ginseng Res 2015: 39: 322–330.

[31] Tyrrell R M. Activation of mammalian gene expression by the UV component of sunlight--from models to reality. Bioessays 1996: 18: 139–148.

[32] Slominski A T, Li W, Kim T K, Semak I, Wang J, Zjawiony J K, Tuckey R C. Novel activities of CYP11A1 and their potential physiological significance. J Steroid Biochem Mol Biol 2015: 151: 25-37.

[33] Slominski A, Zjawiony J, Wortsman J, Semak I, Stewart J, Pisarchik A, Sweatman T, Marcos J, Dunbar C, Tuckey R C. A novel pathway for sequential transformation of 7-dehydrocholesterol and expression of the P450scc system in mammalian skin. Eur J Biochem 2004: 271: 4178-4188.

[34] Slominski A, Zbytek B, Nikolakis G, Manna P R, Skobowiat C, Zmijewski M, Li W, Janjetovic Z, Postlethwaite A, Zouboulis C C, Tuckey R C. Steroidogenesis in the skin: implications for local immune functions. J Steroid Biochem Mol Biol 2013: 137: 107-123.[35] Arck P C, Slominski A, Theoharides T C, Peters E M J, Paus R. Neuroimmunology of stress: skin takes center stage. J Invest Dermatol 2006: 126: 1697–1704.

[36] Hengge U R, Ruzicka T, Schwartz R A, Cork M J. Adverse effects of topical glucocorticosteroids. J Am Acad Dermatol 2006: 54: 1–15.

[37] Nuutinen P, Riekki R, Parikka M et al. Modulation of collagen synthesis and mRNA by continuous and intermittent use of topical hydrocortisone in human skin. Br J Dermatol 2003: 148: 39–45.

[38] Odermatt A, Nashev L G. The glucocorticoid-activating enzyme 11β-hydroxysteroid dehydrogenase type 1 has broad substrate specificity: physiological and toxicological considerations. J Steroid Biochem Mol Biol 2010: 119: 1–13.

[39] Wlaschek M, Bolsen K, Herrmann G et al. UVA-induced autocrine stimulation of fibroblast-derived-collagenase by IL-6: a possible mechanism in dermal photodamage? J Invest Dermatol 1993: 101:164–168.

[40] Wlaschek M, Heinen G, Poswig A, Schwarz A, Krieg T, Scharffetter-Kochanek K. UVA-induced autocrine stimulation of fibroblast-derived collagenase/MMP-1 by interrelated loops of interleukin-1 and interleukin-6. Photochem Photobiol 1994: 59: 550–556.

[41] Cho S, Shin M H, Kim Y K et al. Effects of infrared radiation and heat on human skin aging in vivo. J Investig Dermatol Symp Proc 2009: 14: 15–19.

[42] Wilckens T. Glucocorticoids and immune function: physiological relevance and pathogenic potential of hormonal dysfunction. Trends Pharmacol Sci 1995: 16: 193–197.

[43] Shin B K, Kwon S W, Park J H. Chemical diversity of ginseng saponins from Panax ginseng. J Ginseng Res 2015: 39: 287–298.

Figure Legends

Figure 1. Effects of GERg3 on 11β-HSD1 mRNA expression and cortisol secretion. (a) 11β-HSD1 mRNA expression and (b) cortisol secretion in UVB-exposed cultured human dermal fibroblasts (Hs68 cells) (n = 3). Both 11β-HSD1 mRNA expression and cortisol secretion were decreased by 0.1 ppm and 1 ppm of GERg3 in UVB-exposed human dermal fibroblasts (Hs68 cells). (-): UVB-protected control, (+): UVB-exposed control, PF: PF915275 (11β-HSD1 specific inhibitor). $^{\#\#}P < 0.01$ indicates a significant difference from UVB-protected control. $^{*}P < 0.05$ or $^{**}P < 0.01$ indicates a significant difference from UVB-exposed control.

Figure 2. Effects of GERg3 on IL-6, MMP-1, and type 1 procollagen expressions. (a) IL-6 mRNA expression, (b) IL-6 secretion. (c) MMP-1 mRNA expression, (d) MMP-1 protein expression, (e) col1α1 mRNA expression, and (f) type 1 procollagen expression in UVB-exposed cultured Human dermal fibroblasts (Hs68 cells) (n = 3). Both IL-6 mRNA expression and IL-6 secretion were decreased by 0.1 ppm and 1 ppm of GERg3 in UVB-exposed Human dermal fibroblasts (Hs68 cells). Both MMP-1 mRNA and protein expressions were decreased by 0.1 ppm and 1 ppm of GERg3 in UVB-exposed Human dermal fibroblasts (Hs68 cells). Both col1α1 mRNA expression and type 1 procollagen production were recovered by 0.1 ppm and 1 ppm of GERg3 in UVB-exposed Human dermal fibroblasts (Hs68 cells). (-): UVB-protected control, (+): UVB-exposed control, PF: PF915275 (11β-HSD1 specific inhibitor). $^{\#\#}P < 0.01$ indicates a significant difference from

UVB-protected control. $^{**}P < 0.01$ indicates a significant difference from UVB-exposed control.

Figure 3. Effects of GERg3 on 11β-HSD1 mRNA expression and cortisol secretion. (a) 11β-HSD1 mRNA expression and (b) cortisol secretion in IR-exposed cultured Human dermal fibroblasts (Hs68 cells) (n = 3). Both 11β-HSD1 mRNA expression and cortisol secretion were decreased by 0.1 ppm and 1 ppm of GERg3 in IR-exposed Human dermal fibroblasts (Hs68 cells). (-): IR-protected control, (+): IR-exposed control, PF: PF915275 (11β-HSD1 specific inhibitor). $^{\#\#}P < 0.01$ indicates a significant difference from IR-protected control. $^{*}P < 0.05$ or $^{**}P < 0.01$ indicates a significant difference from IR-exposed control.

Figure 4. Effects of GERg3 on IL-6, MMP-1, and type 1 procollagen expressions. (a) IL-6 mRNA expression, (b) IL-6 secretion. (c) MMP-1 mRNA expression, (d) MMP-1 protein expression, (e) col1α1 mRNA expression, and (f) type 1 procollagen expression in IR-exposed cultured Human dermal fibroblasts (Hs68 cells) (n = 3). Both IL-6 mRNA expression and IL-6 secretion were decreased by 0.1 ppm and 1 ppm of GERg3 in IR-exposed Human dermal fibroblasts (Hs68 cells). Both MMP-1 mRNA and protein expressions were decreased by 0.1 ppm and 1 ppm of GERg3 in IR-exposed Human dermal fibroblasts (Hs68 cells). Both col1α1 mRNA expression and type 1 procollagen production were recovered by 0.1 ppm and 1 ppm of GERg3 in IR-exposed Human dermal fibroblasts (Hs68 cells). (-): IR-protected control, (+): IR-exposed control, PF: PF915275 (11β-HSD1 specific inhibitor). $^{\#\#}P < 0.01$ indicates a significant difference from IR-protected control. $^{*}P < 0.05$ or $^{**}P < 0.01$ indicates a significant difference from IR-exposed control.

Figure 5. Effects of GERg3 on changes of normal human 3D skin model. (a) cortisol secretion, (b) IL-6 secretion, (c) MMP-1 expression, (d) type 1 procollagen production, and (e) dermal thickness in UVA-exposed 3D skin model. Cortisol and IL-6 secretion, and MMP-1 expression were decreased by 0.1 ppm and 1 ppm of GERg3 in UVA-exposed 3D skin model. Type 1 procollagen production was recovered by 0.1 ppm and 1 ppm of GERg3 in UVA-exposed 3D skin model. UVA-induced decrease of dermal thickness was recovered by 1 ppm of GERg3 in 3D skin model. (-): UVA-protected control, (+): UVA-exposed control, PF: PF915275 (11β-HSD1 specific inhibitor). $^{\#\#}P < 0.01$ indicates a significant difference from UVA-protected control. $^{*}P < 0.05$ or $^{**}P < 0.01$ indicates a significant difference from UVA-exposed control.

Supplementary figure 1. HPLC chromatogram of ginsenoside Rg3(S) in GERg(3). (a) The peak of Rg3(S) standard was detected at retention time 40.944 min. (b) The peak regarded as the peak of Rg3(S) was detected at retention time 40.981 min. In comparison with Figure 1A, the retention time difference is about 0.037 min. This gap is about 0.090 % comparing with the retention time (RT) of the standard reagent and it is negligible. This gap in RT is depending on performance of the apparatus. (c) The UV spectrum can be confirmed in GERg(3) and Rg3(S) standard reagent. This means that the peaks have same maximum absorption wavelength and the both are same materials.

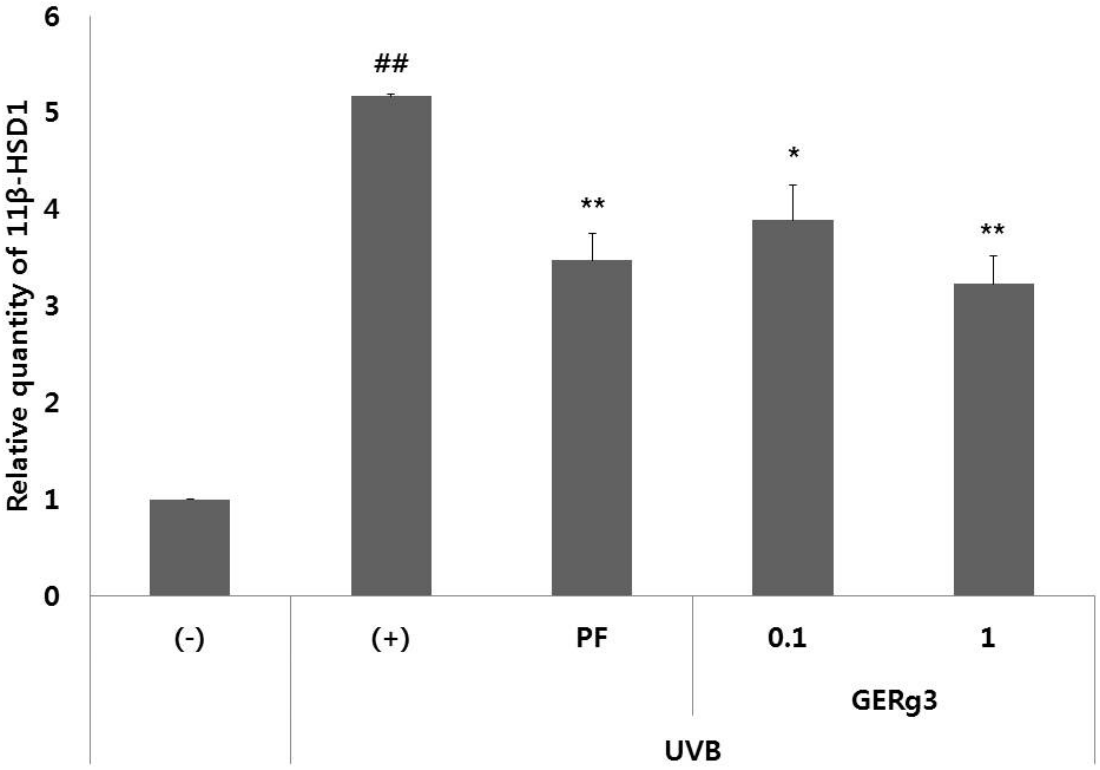

Figure 1a

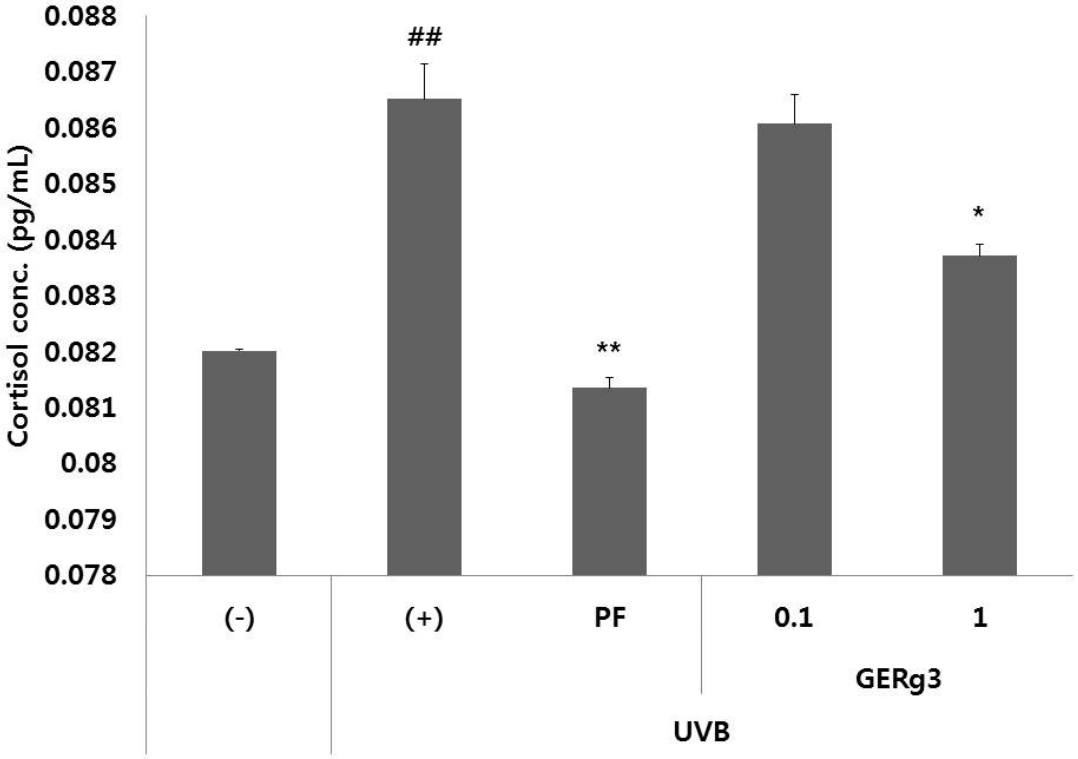

Figure 1b

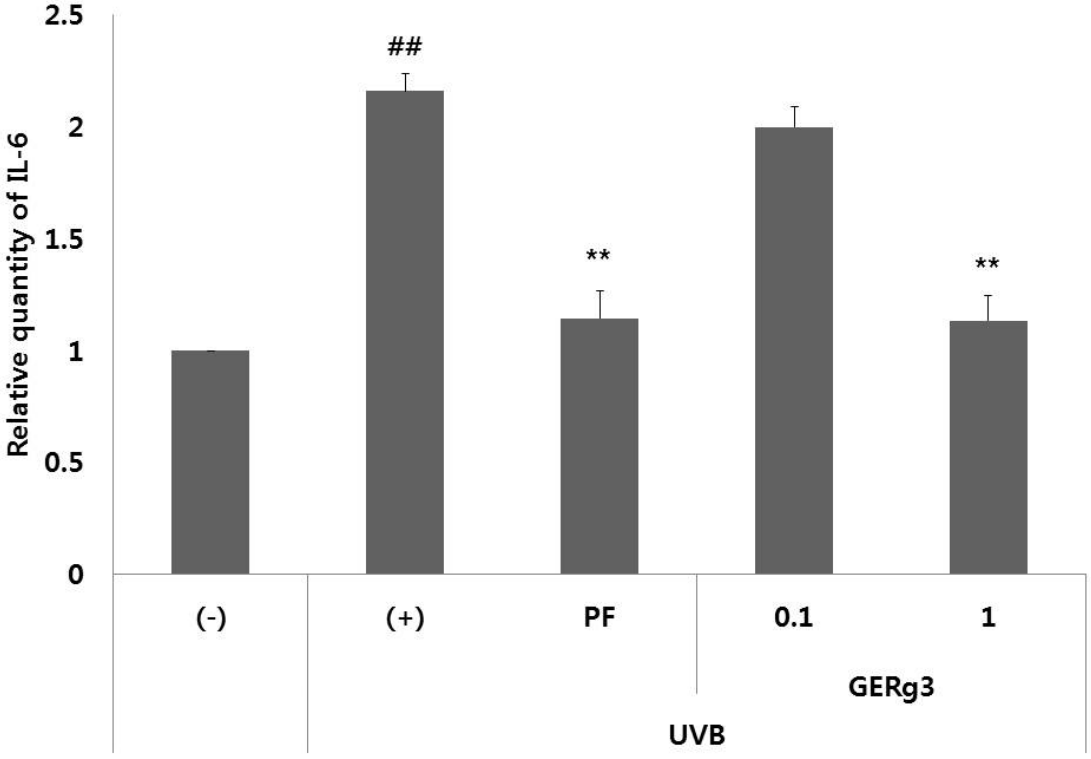

Figure 2a

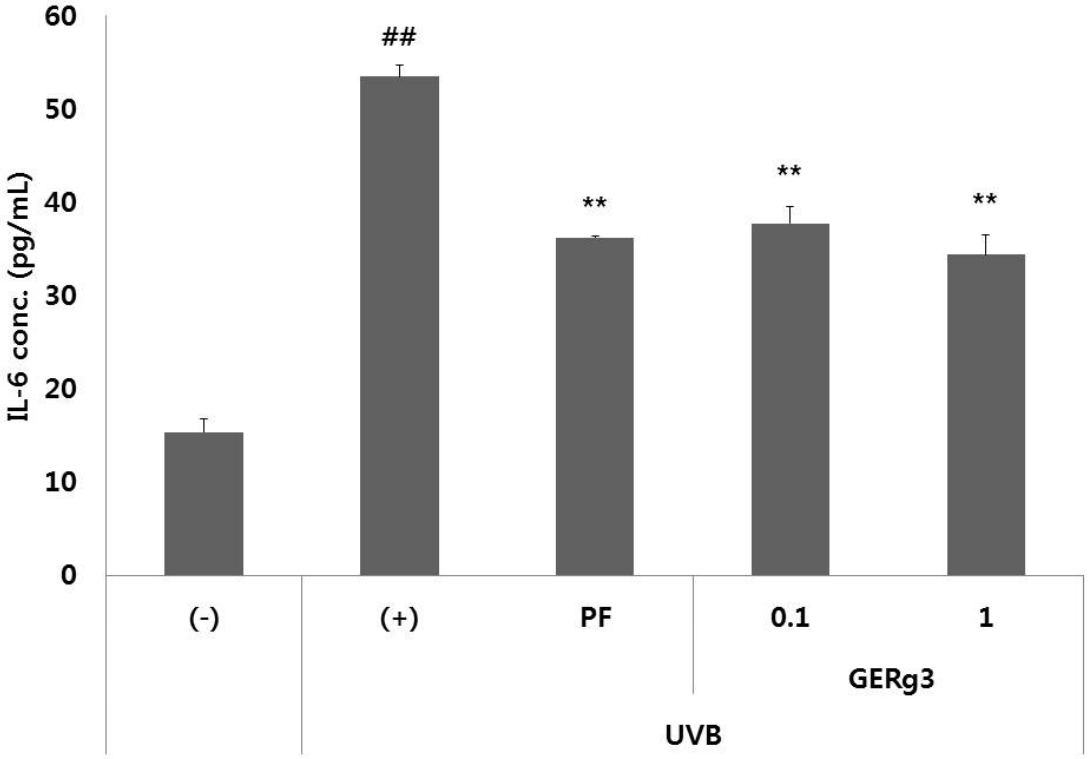

Figure 2b

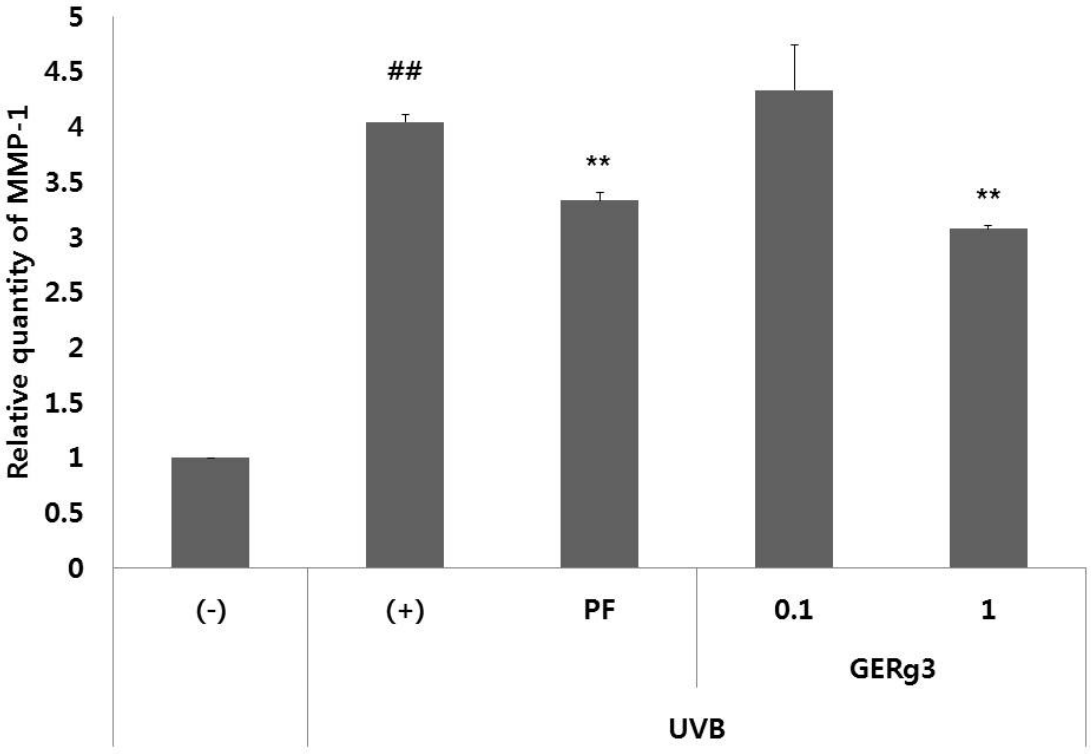

Figure 2c

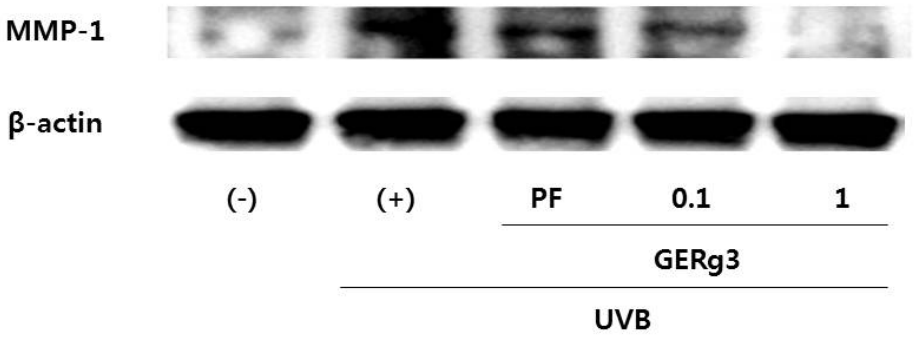

Figure 2d

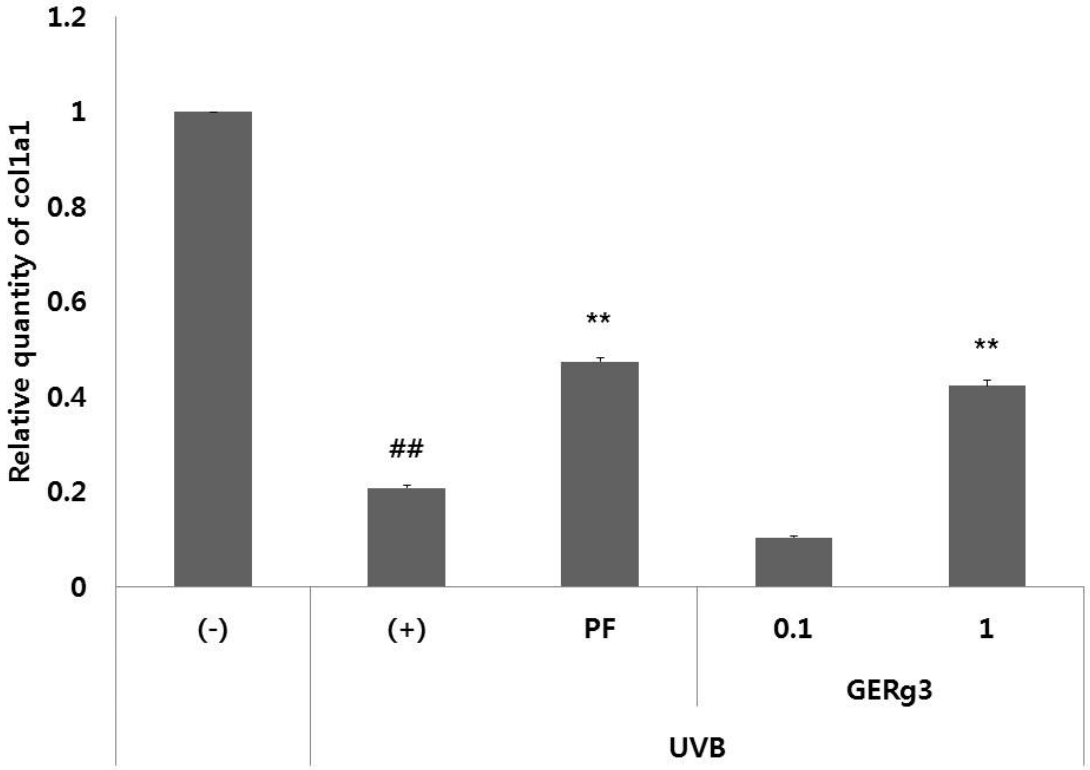

Figure 2e

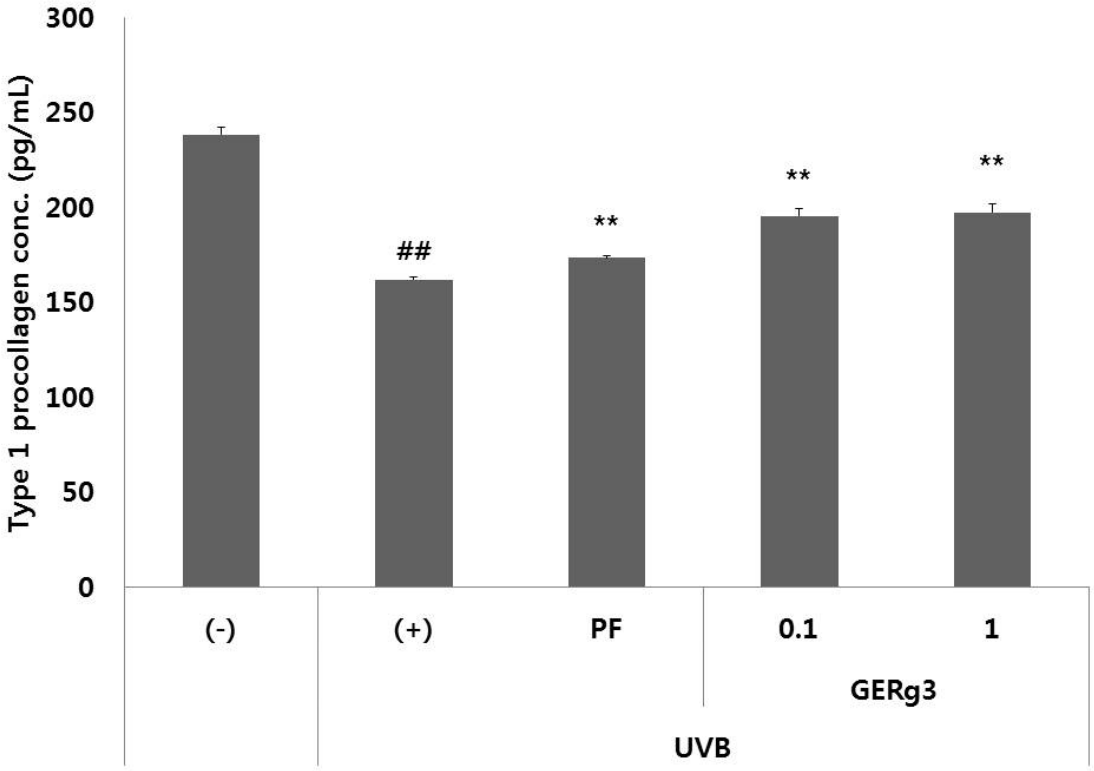

Figure 2f

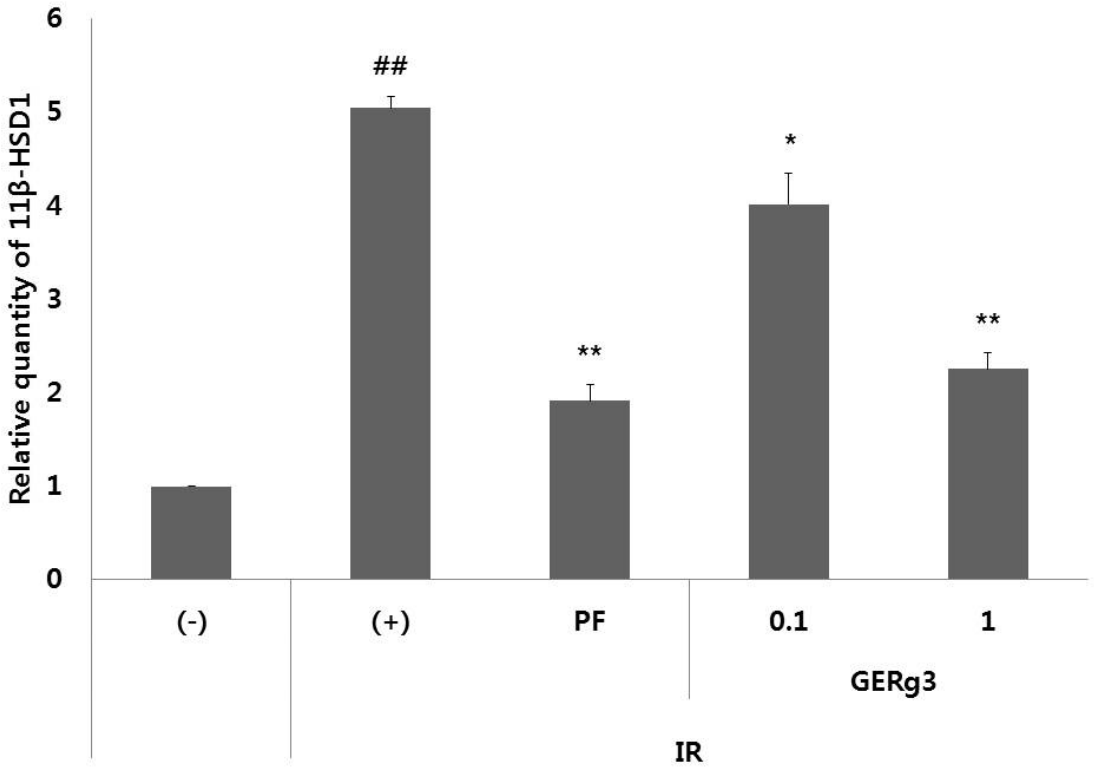

Figure 3a

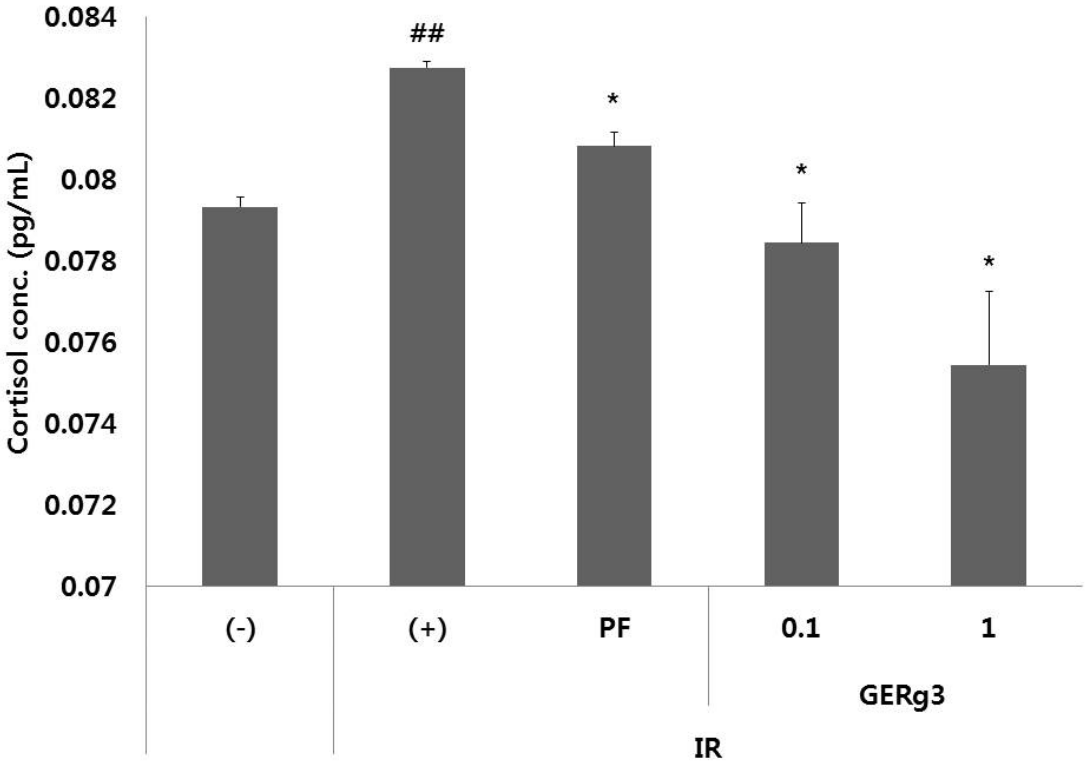

Figure 3b

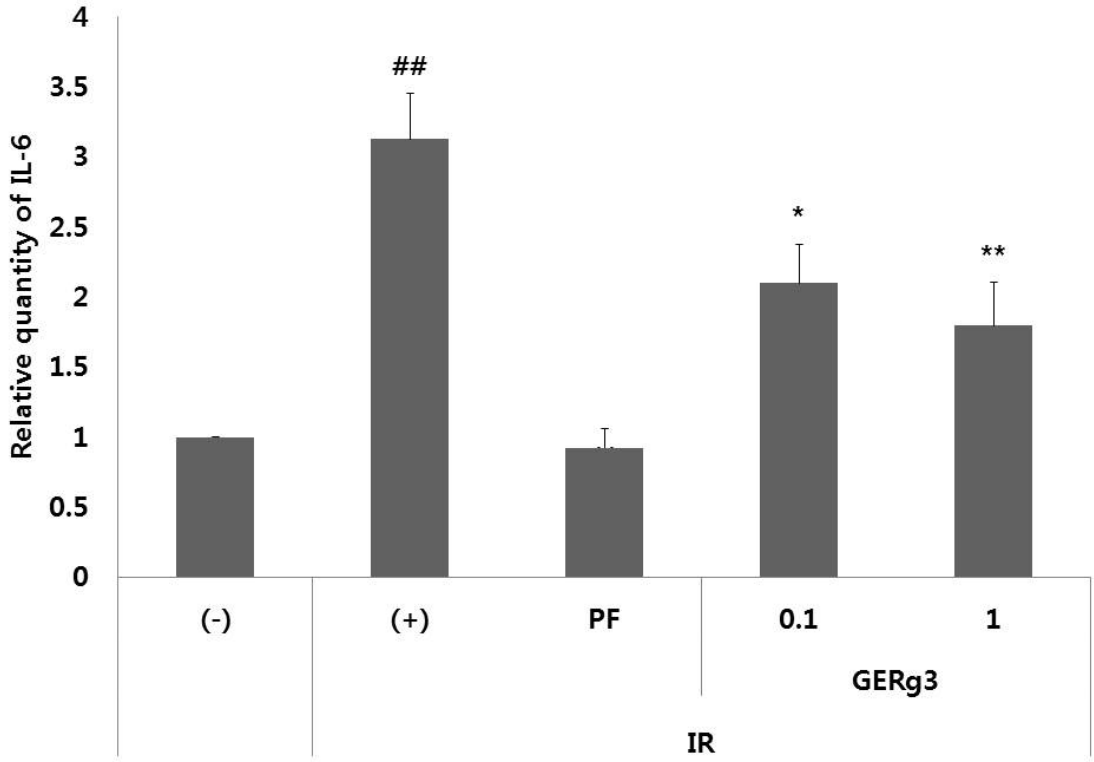

Figure 4a

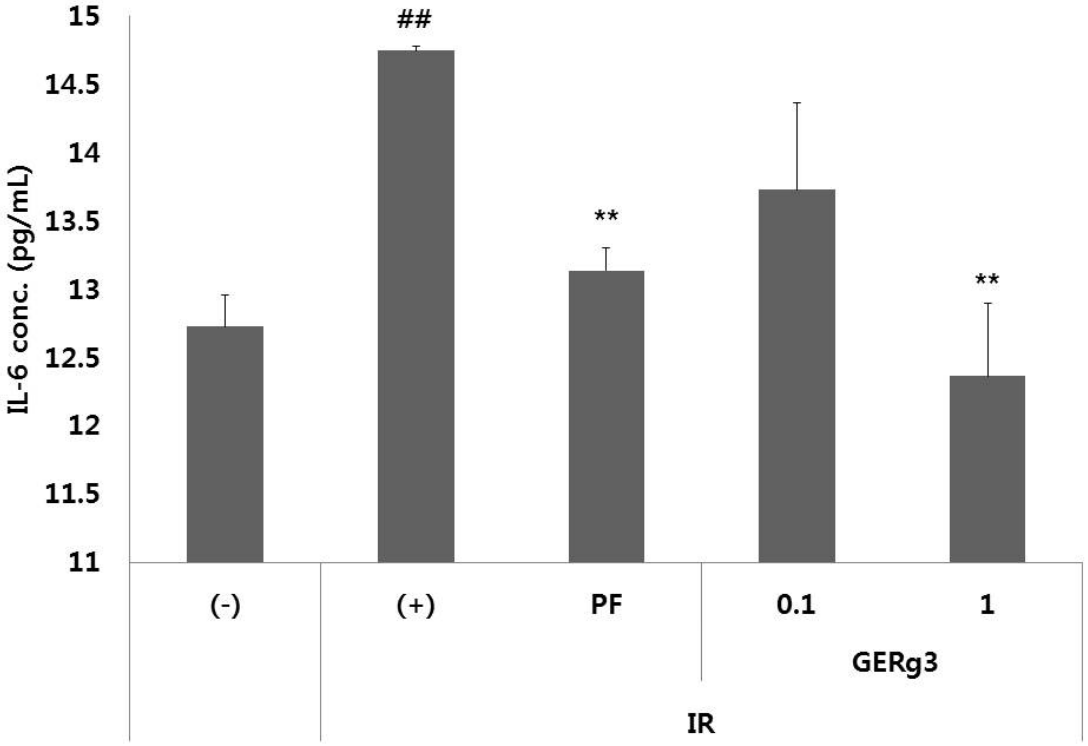

Figure 4b

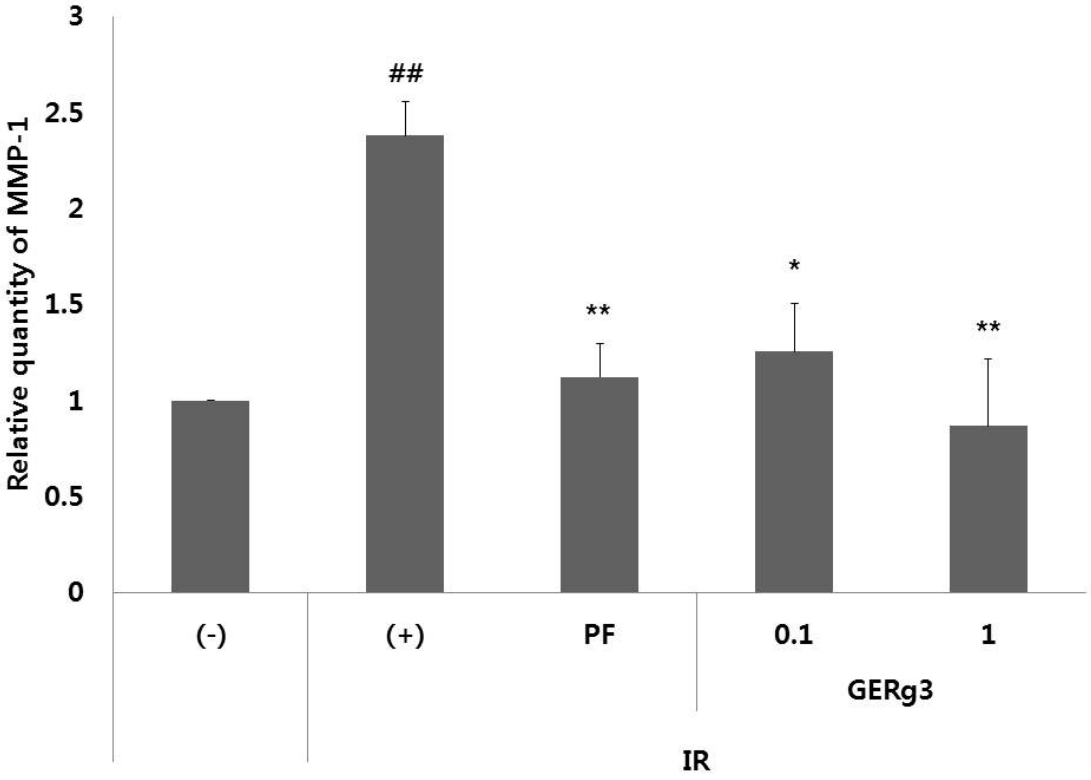

Figure 4c

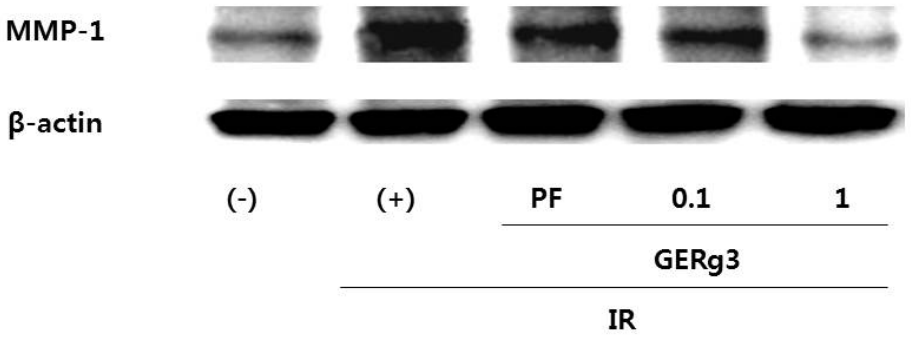

Figure 4d

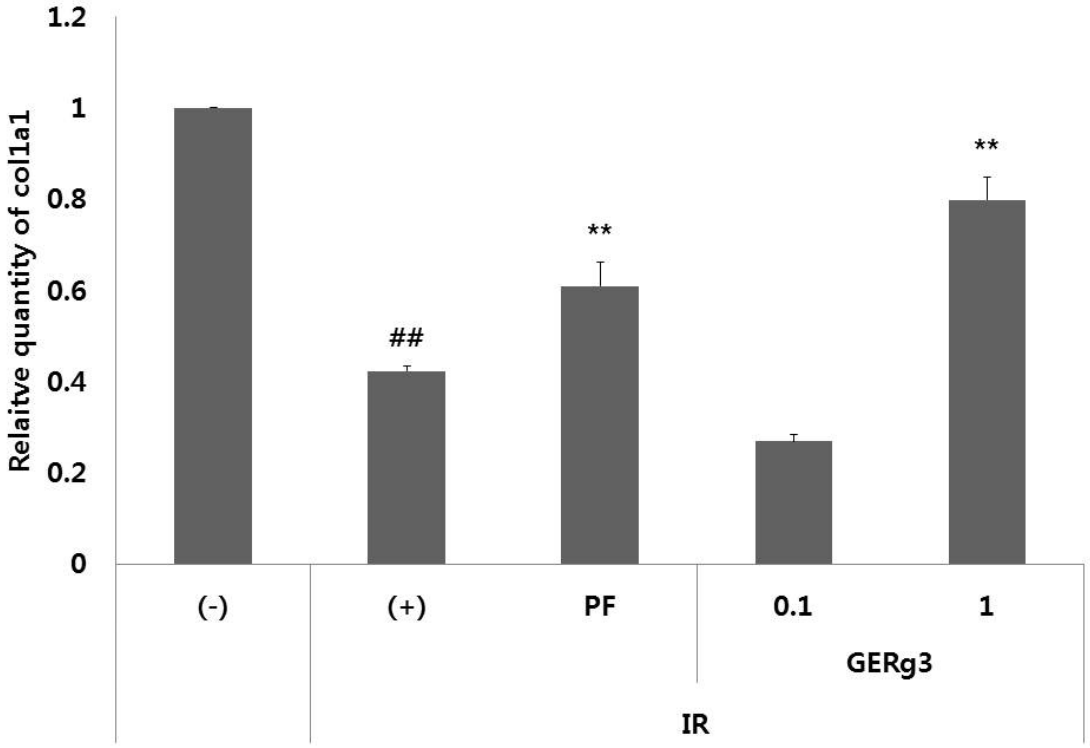

Figure 4e

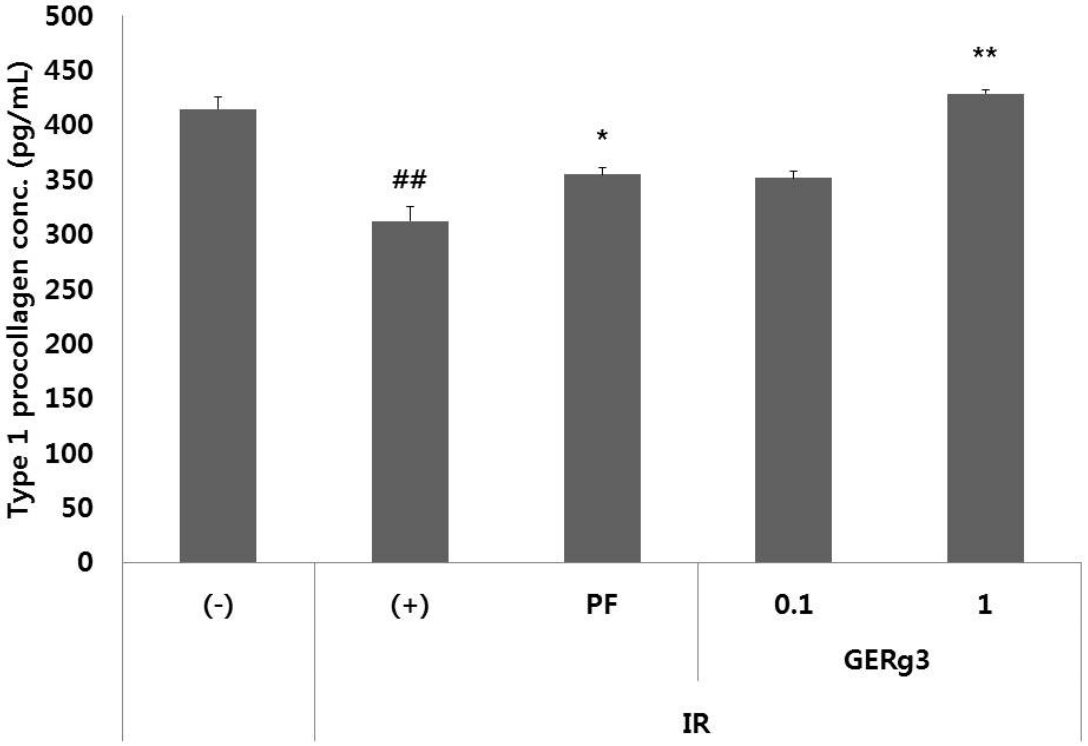

Figure 4f

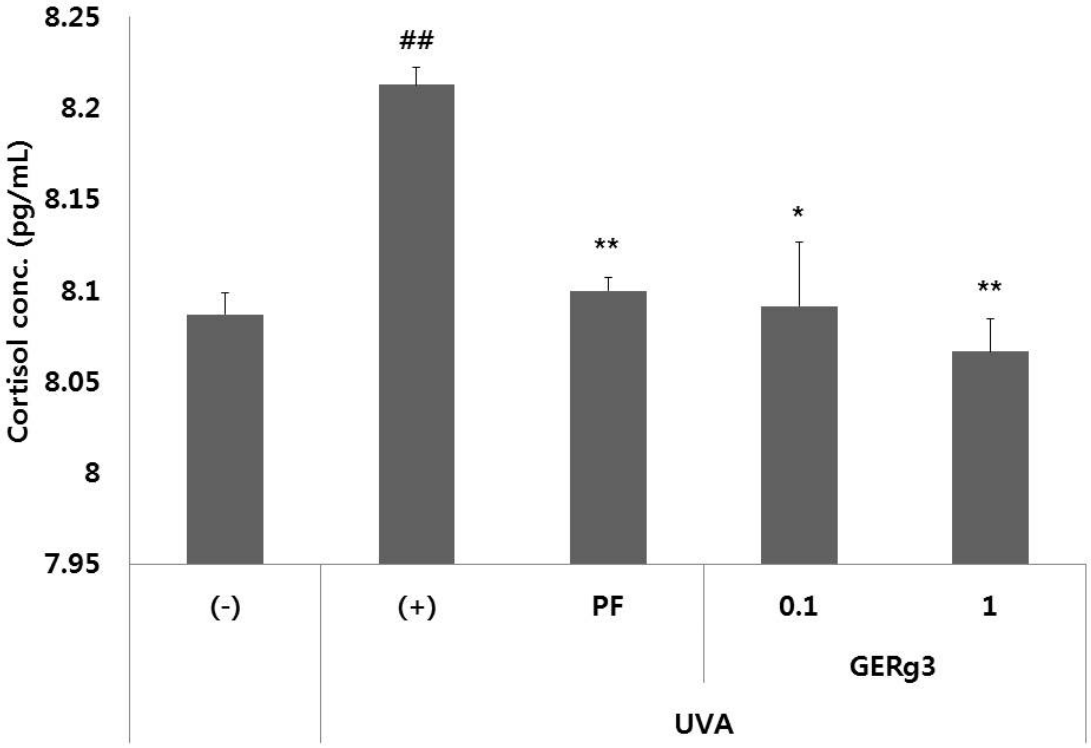

Figure 5a

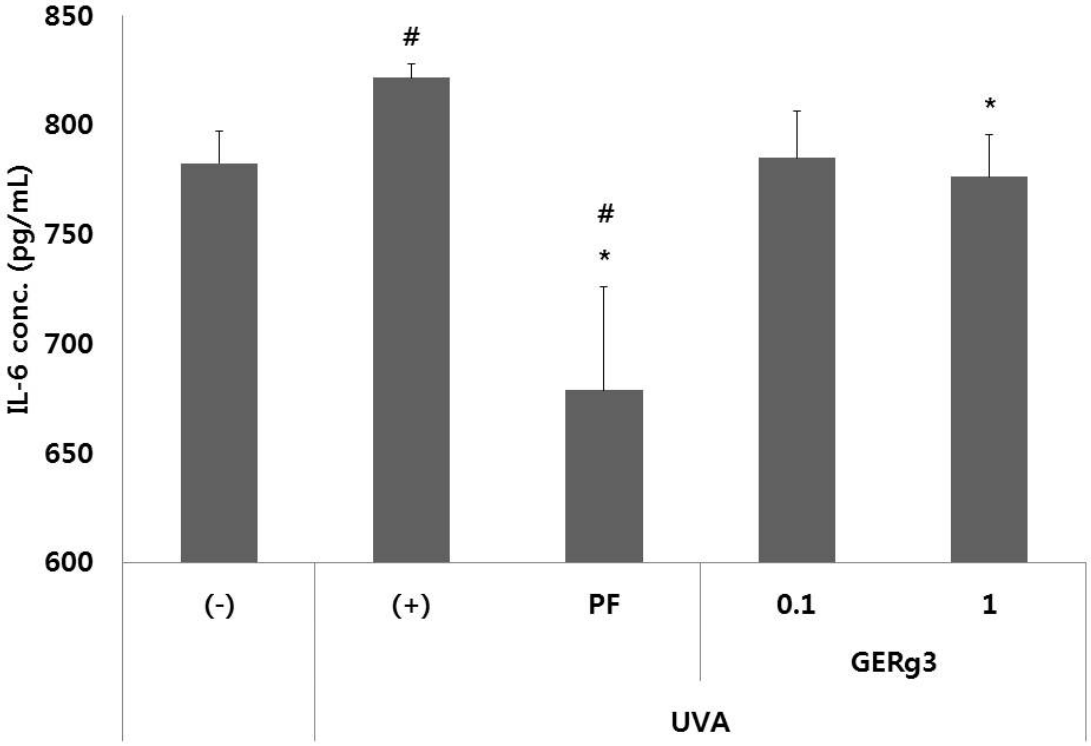

Figure 5b

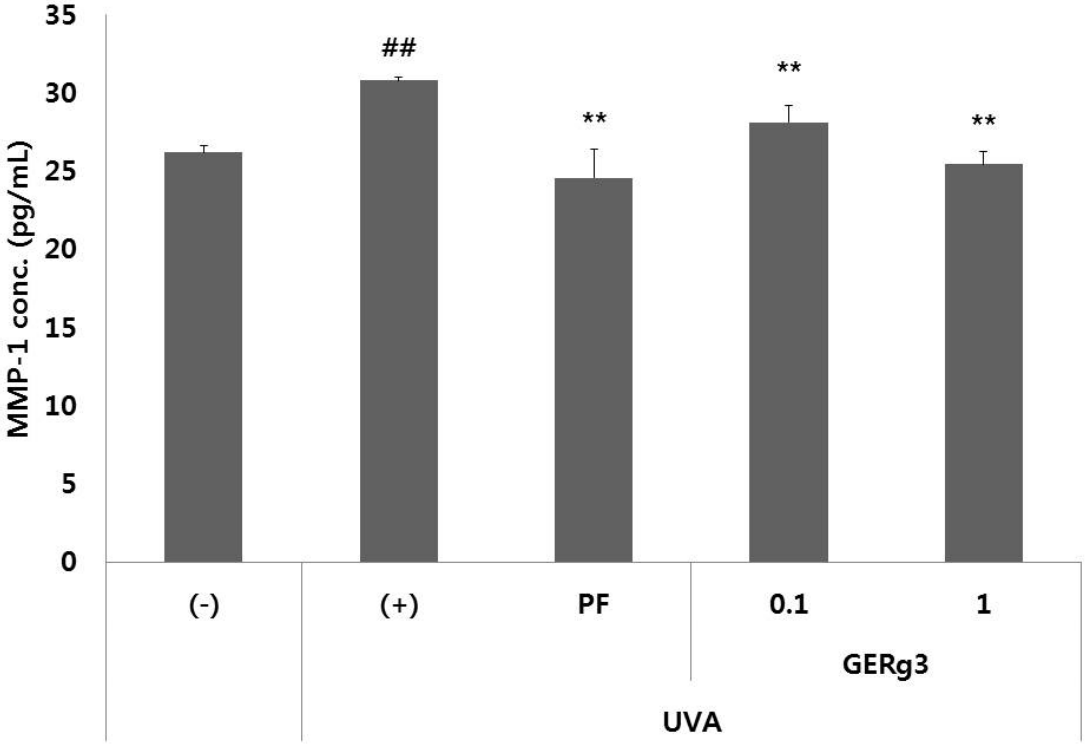

Figure 5c

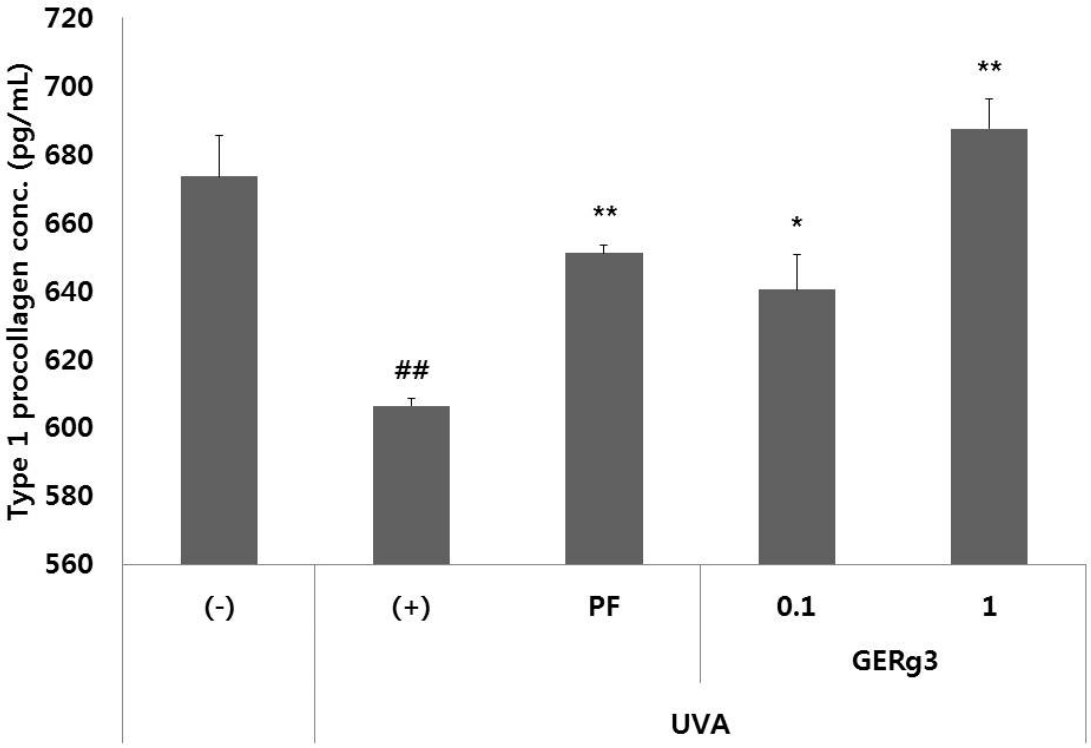

Figure 5d

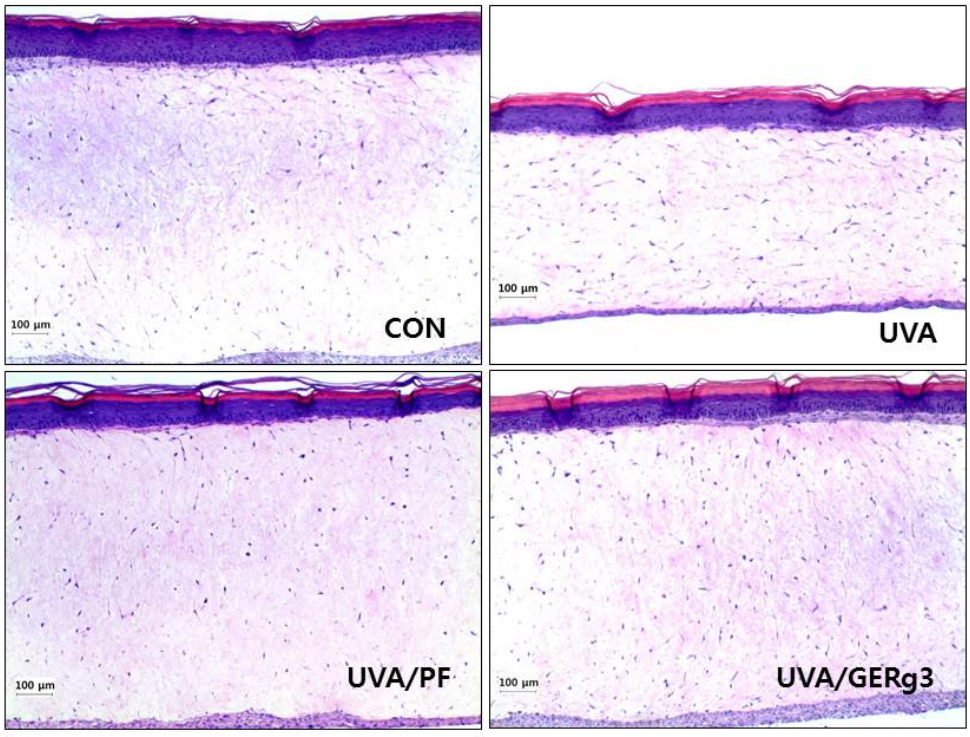

Figure 5e